

**Presentation for ICCE 2018(Jul31, 2018)**

# **A two-layer non-hydrostatic landslide model for tsunami generation on irregular bathymetry**

Cheng Zhang<sup>1</sup>, James T. Kirby<sup>1</sup>, Stéphan T. Grilli<sup>2</sup>, Fengyan Shi<sup>1</sup>, Gangfeng Ma<sup>3</sup>

1. Center for Applied Coastal Research, University of Delaware, Newark, DE 19716, USA
2. Department of Ocean Engineering, University of Rhode Island, Narragansett, RI 02882, USA
3. Department of Civil and Environmental Engineering, Old Dominion University, Norfolk, VA 23529, USA



# Introduction

## □ Motivation:

1. Landslide (or S(ubmarine) M(ass) F(ailure)s) can have catastrophic impacts on coastal communities and infrastructure;

2. Treatment of SMFs as rigid slides or slumps can lead to overly conservative predictions during hazard analysis;

3. A more representative deformable slide model for SMFs is needed ;

4. Classification is related to the choice of flow rheology in numerical simulation;

5. Type I, **mudflow**;

6. Type II, **granular flow**.

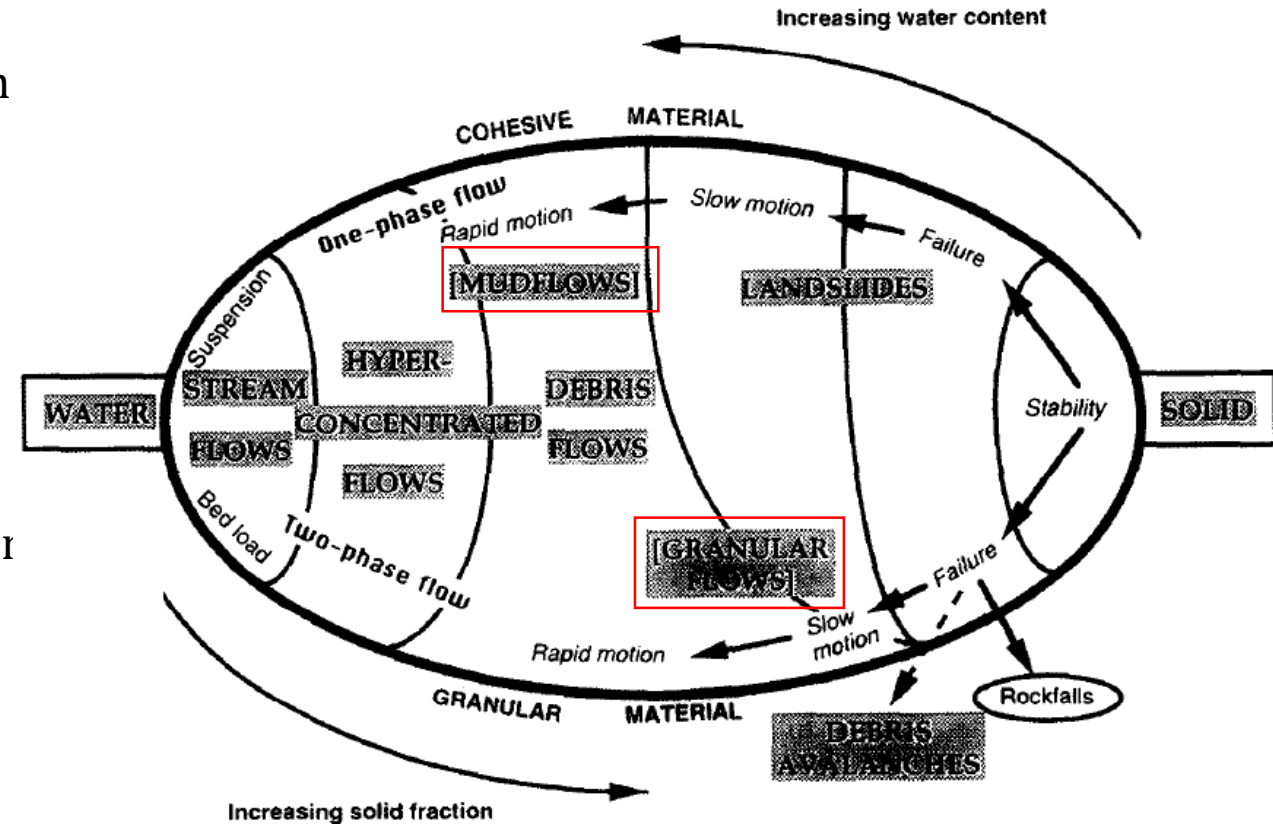


Figure 1: Classification of flowing mass. (From Coussot and Meunier 1996)

# Introduction

## □ Two-layer landslide model :

1. The model consists of two models for different layers;
2. Non-hydrostatic wave model NHWAVE is used for upper-layer wave (Ma et al. 2012; Derakhti et al. 2016);
3. Non-hydrostatic shallow-water type model with various rheology closures for lower-layer landslide.

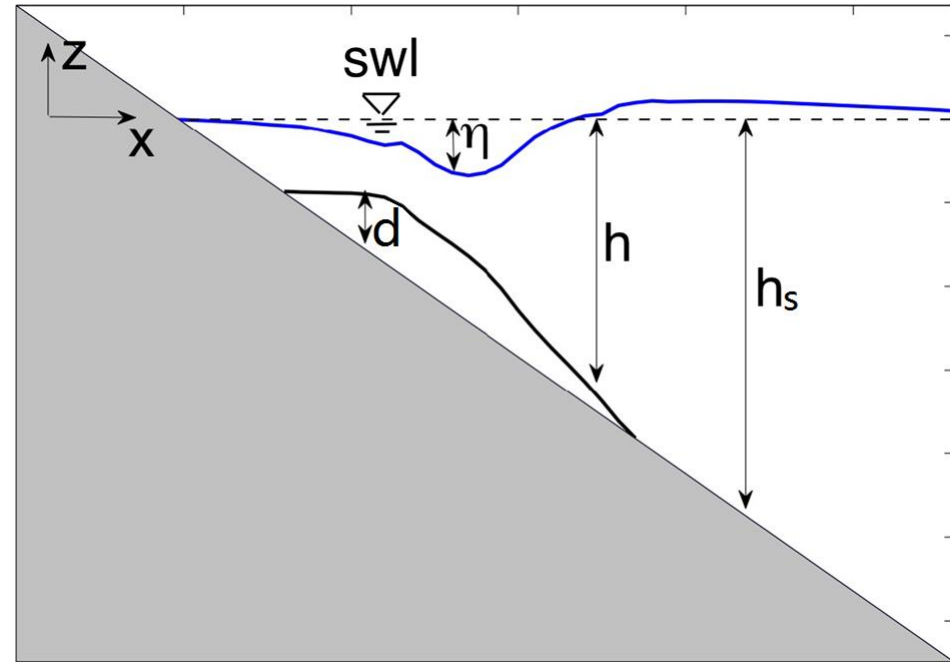


Figure 2: Sketch for two-layer landslide model. (From Grilli et al. 2017)

# Introduction

## □ Shallow water regime:

1. Flowing mass has fluid-like manner (Savage and Hutter 1989);
2. Ratio of slide thickness  $D$  and length  $L$  is much smaller than 1;

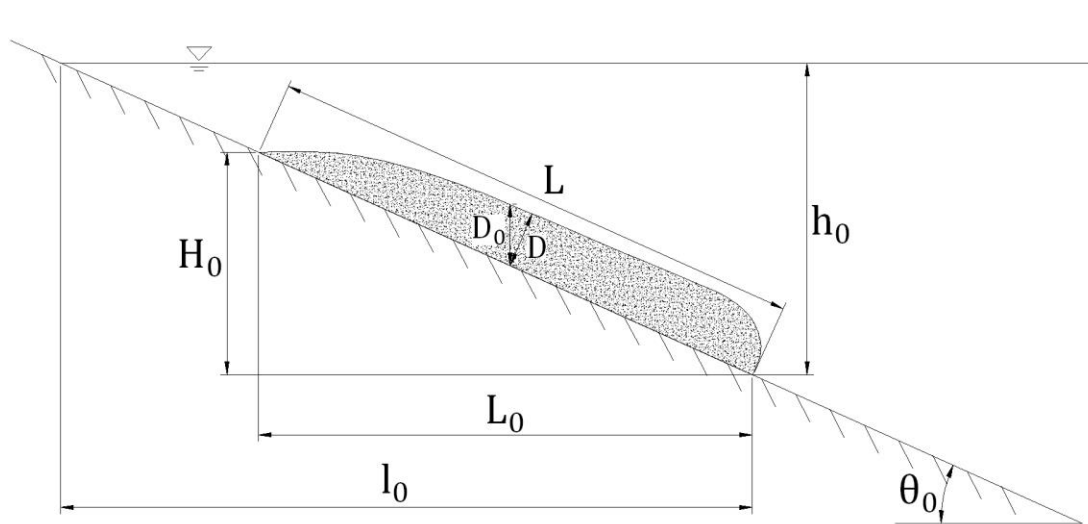


Figure 3: Characteristic lengths of flowing mass.

## □ Coordinate system:

1. SMF occurs on irregular bathymetry;
2. Three coordinate systems;
3. Regular Cartesian coordinate is adopted;

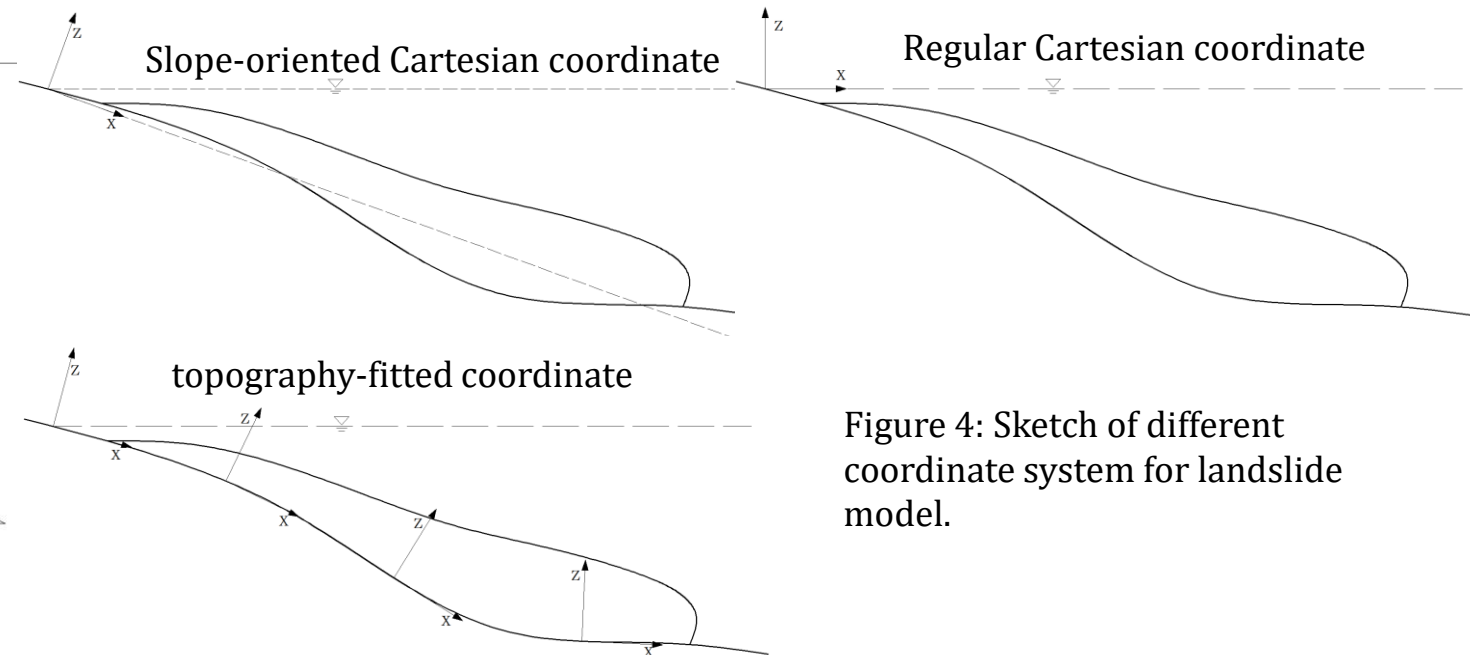


Figure 4: Sketch of different coordinate system for landslide model.

# Theoretical Background

## □ Conservation laws:

1. Governing equations for solid-phase and fluid-phase are:

$$\frac{\partial \rho_s \phi}{\partial t} + \nabla \cdot (\rho_s \phi \mathbf{v}_s) = 0$$

$$\frac{\partial \rho_f (1 - \phi)}{\partial t} + \nabla \cdot (\rho_f (1 - \phi) \mathbf{v}_f) = 0$$

$$\frac{\partial \rho_s \phi \mathbf{v}_s}{\partial t} + \nabla \cdot (\rho_s \phi \mathbf{v}_s \mathbf{v}_s) = \nabla \cdot \mathbf{T}_s - \nabla \cdot p_s + \rho_s \phi \mathbf{g} + \mathbf{f}$$

$$\frac{\partial \rho_f (1 - \phi) \mathbf{v}_f}{\partial t} + \nabla \cdot (\rho_f (1 - \phi) \mathbf{v}_f \mathbf{v}_f) = \nabla \cdot \mathbf{T}_f - \nabla \cdot p_f + \rho_f (1 - \phi) \mathbf{g} - \mathbf{f}$$

2. Sum them up and obtain equations for mixture mass and momentum conservation:

$$\frac{\partial \rho}{\partial t} + \nabla \cdot (\rho \mathbf{v}) = 0$$

$$\frac{\partial \rho \mathbf{v}}{\partial t} + \nabla \cdot (\rho \mathbf{v} \mathbf{v}) = \nabla \cdot \mathbf{T} - \nabla \cdot p + \rho \mathbf{g} \quad \text{where} \quad \rho = \rho_s \phi + \rho_f (1 - \phi) \quad \mathbf{v} = (\rho_s \phi \mathbf{v}_s + \rho_f (1 - \phi) \mathbf{v}_f) / \rho \quad \mathbf{T} = \mathbf{T}_s + \mathbf{T}_f$$

$$\mathbf{v}_f - \mathbf{v}_s \quad \text{slip velocity} \quad p = p_s + p_f$$

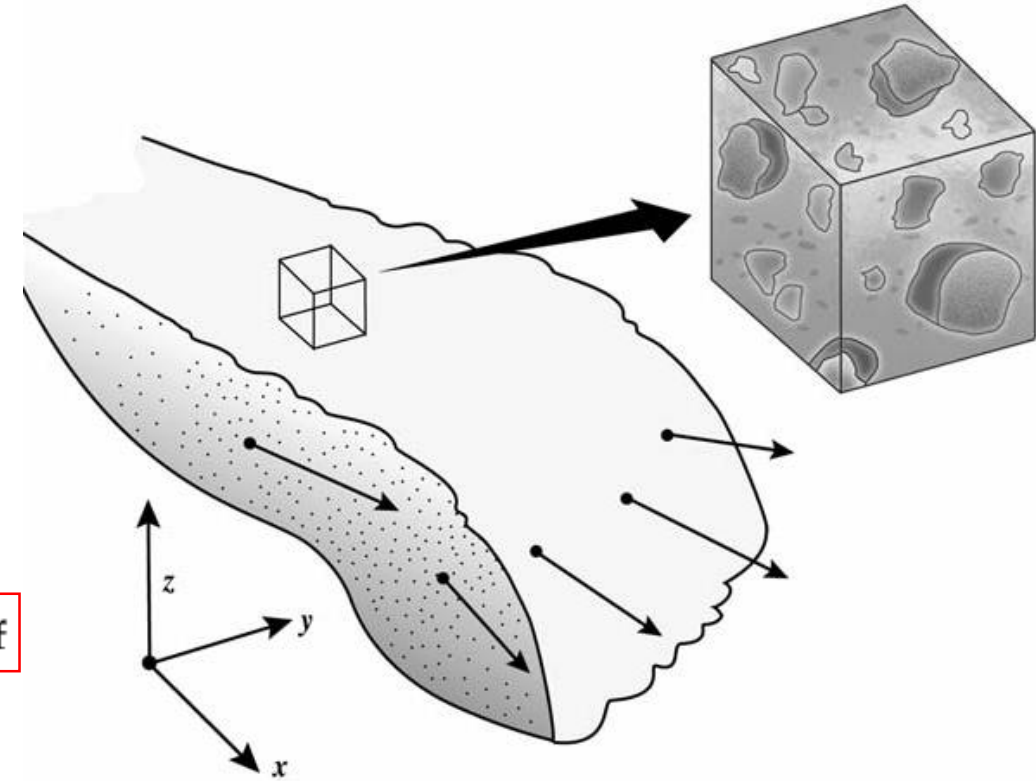


Figure 5: Sketch of landslide flow. (From Iverson 2005).

## Theoretical Background

3. In the regular Cartesian coordinates system  $(x, y, z)$ , the conservation equations can be rewritten as

$$\begin{aligned} \frac{\partial \rho}{\partial t} + \frac{\partial \rho u_\beta}{\partial x_\beta} + \frac{\partial \rho w}{\partial z} &= 0 \\ \frac{\partial \rho u_\alpha}{\partial t} + \frac{\partial \rho u_\alpha u_\beta}{\partial x_\beta} + \frac{\partial \rho u_\alpha w}{\partial z} &= \frac{\partial \tau_{\beta\alpha}}{\partial x_\beta} + \frac{\partial \tau_{z\alpha}}{\partial z} - \frac{\partial p}{\partial x_\alpha} \\ \frac{\partial \rho w}{\partial t} + \frac{\partial \rho w u_\beta}{\partial x_\beta} + \frac{\partial \rho w^2}{\partial z} &= \frac{\partial \tau_{\beta z}}{\partial x_\beta} + \frac{\partial \tau_{zz}}{\partial z} - \frac{\partial p}{\partial z} - \rho g \end{aligned}$$

Kinematic boundary conditions (KBCs) for the equations are

$$\begin{aligned} \frac{\partial h}{\partial t} + u_\beta(-h) \frac{\partial h}{\partial x_\beta} + w(-h) &= 0 \\ \frac{\partial h_s}{\partial t} + u_\beta(-h_s) \frac{\partial h_s}{\partial x_\beta} + w(-h_s) &= 0 \end{aligned}$$

Traction-free boundary condition is used in the current version of model.

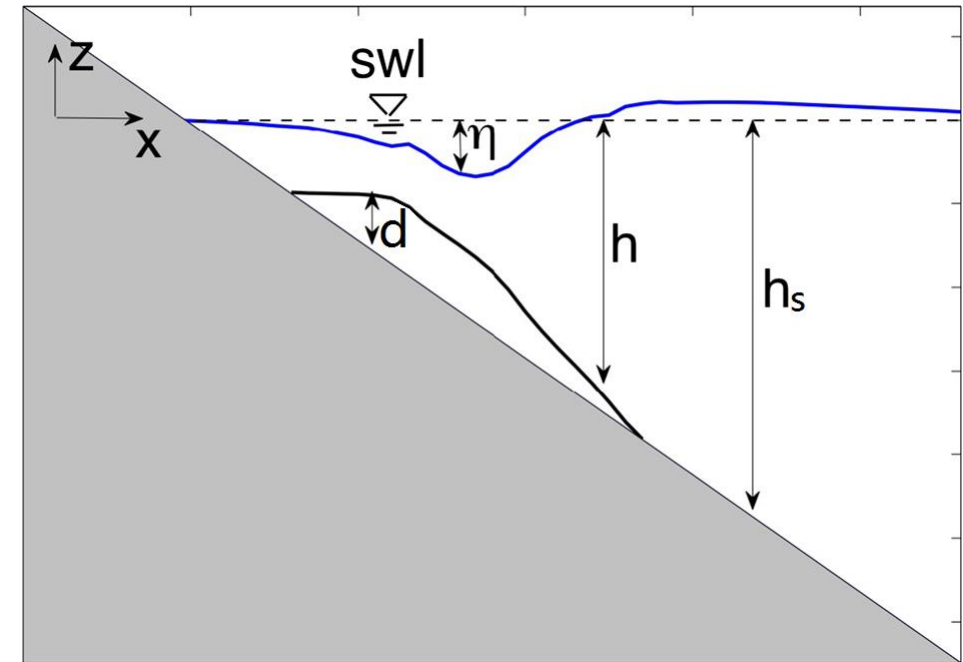


Figure 6: Definition sketch for underwater landslide. (From Grilli et al. 2017)

# Theoretical Background

## □ Assumptions:

1.  $\rho$  is vertically uniform;
2. Vertical velocity is linear in vertical;
3.  $\bar{q} = 2/3 (q(-h_s) + q(-h))$  is imposed to ensure a correct linear dispersion relation;
5. In z momentum equation, assume vertical normal stress is dominant and advective effect is small;
6. No water and soil exchange;
7. Constant porosity and mixture density.

# Theoretical Background

□ Depth-averaged equations:

**Mass:**

$$\frac{\partial \rho d}{\partial t} + \frac{\partial \rho \bar{u}_\beta d}{\partial x_\beta} = 0$$

**x/y-momentum:**

$$\frac{\partial \rho \bar{u}_\alpha d}{\partial t} + \frac{\partial \Gamma_{\alpha\beta} \rho \bar{u}_\alpha \bar{u}_\beta d}{\partial x_\beta} = \frac{\partial \bar{\tau}_{\beta\alpha} d}{\partial x_\beta} + \tau_{\beta\alpha}(-h) \frac{\partial h}{\partial x_\beta} + \tau_{z\alpha}(-h) - \tau_{\beta\alpha}(-h_s) \frac{\partial h_s}{\partial x_\beta} - \tau_{z\alpha}(-h_s)$$

$$- \rho_f g d \frac{\partial(\eta + h)}{\partial x_\alpha} \quad \left| \quad - \frac{1}{2} g \frac{\partial \rho d^2}{\partial x_\alpha} + \rho g d \frac{\partial h_s}{\partial x_\alpha} \right.$$

$$\left. - \frac{2}{3} \frac{\partial q(-h)d}{\partial x_\alpha} - q(-h) \frac{\partial h}{\partial x_\alpha} - \frac{2}{3} \frac{\partial q(-h_s)d}{\partial x_\alpha} + q(-h_s) \frac{\partial h_s}{\partial x_\alpha} \right.$$

**z-momentum:**

$$\frac{\partial \rho \bar{w} d}{\partial t} = \tau_{zz}(-h) - \tau_{zz}(-h_s) \quad \left| \quad - q(-h) + q(-h_s) \right.$$



# Rheology Closure

□ Laminar flow model (mudflow):

1. Low solid concentration;
2. Newtonian fluid at a low Reynolds number;
3. The influence from solid phase is embodied as an increased viscosity which is significantly higher than water;
4. Parabolic velocity profile:

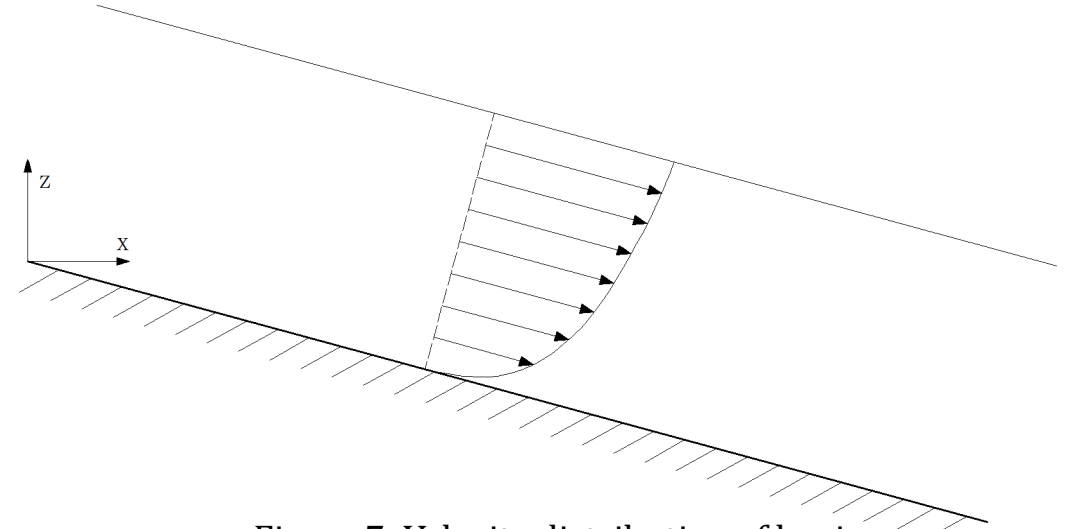


Figure 7: Velocity distribution of laminar open channel flow.

$$\begin{aligned}\tau_{xx}(-h_s) &= 2\mu_e \left. \frac{\partial u}{\partial x} \right|_{\sigma=0} = \frac{6\mu_e \bar{u}}{d} \frac{\partial h_s}{\partial x} \\ \tau_{yy}(-h_s) &= 2\mu_e \left. \frac{\partial v}{\partial y} \right|_{\sigma=0} = \frac{6\mu_e \bar{v}}{d} \frac{\partial h_s}{\partial y} \\ \tau_{zz}(-h_s) &= 2\mu_e \left. \frac{\partial w}{\partial z} \right|_{\sigma=0} = -\frac{2\mu_e}{\rho} \frac{\partial \rho}{\partial t} - \frac{6\mu_e}{d} \left( \bar{u} \frac{\partial h_s}{\partial x} + \bar{v} \frac{\partial h_s}{\partial y} \right) \\ \tau_{xy}(-h_s) &= \tau_{yx}(-h_s) = \mu_e \left( \left. \frac{\partial u}{\partial y} \right|_{\sigma=0} + \left. \frac{\partial v}{\partial x} \right|_{\sigma=0} \right) = \frac{3\mu_e}{d} \left( \bar{u} \frac{\partial h_s}{\partial y} + \bar{v} \frac{\partial h_s}{\partial x} \right)\end{aligned}$$

$$\begin{aligned}\tau_{xz}(-h_s) &= \tau_{zx}(-h_s) = \mu_e \left( \left. \frac{\partial u}{\partial z} \right|_{\sigma=0} + \left. \frac{\partial w}{\partial x} \right|_{\sigma=0} \right) \\ &= \frac{3\mu_e \bar{u}}{d} - \mu_e \frac{\partial^2 h_s}{\partial t \partial x} + \mu_e \frac{\partial E_b \xi_b}{\partial x} - \frac{\mu_e}{\rho} \frac{\partial \rho}{\partial t} \frac{\partial h_s}{\partial x} - \frac{3\mu_e}{d} \left( \bar{u} \frac{\partial h_s}{\partial x} + \bar{v} \frac{\partial h_s}{\partial y} \right) \frac{\partial h_s}{\partial x} \\ \tau_{yz}(-h_s) &= \tau_{zy}(-h_s) = \mu_e \left( \left. \frac{\partial v}{\partial z} \right|_{\sigma=0} + \left. \frac{\partial w}{\partial y} \right|_{\sigma=0} \right) \\ &= \frac{3\mu_e \bar{v}}{d} - \mu_e \frac{\partial^2 h_s}{\partial t \partial y} + \mu_e \frac{\partial E_b \xi_b}{\partial y} - \frac{\mu_e}{\rho} \frac{\partial \rho}{\partial t} \frac{\partial h_s}{\partial y} - \frac{3\mu_e}{d} \left( \bar{u} \frac{\partial h_s}{\partial x} + \bar{v} \frac{\partial h_s}{\partial y} \right) \frac{\partial h_s}{\partial y}\end{aligned}$$

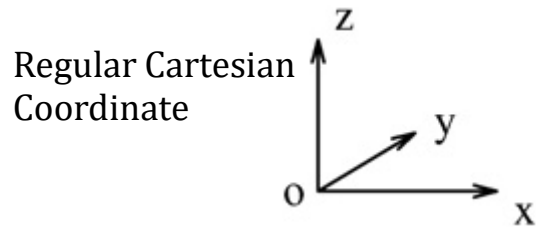
# Rheology Closure

□ Coulomb friction model (granular flow):

1. High solid concentration, low Reynolds number;

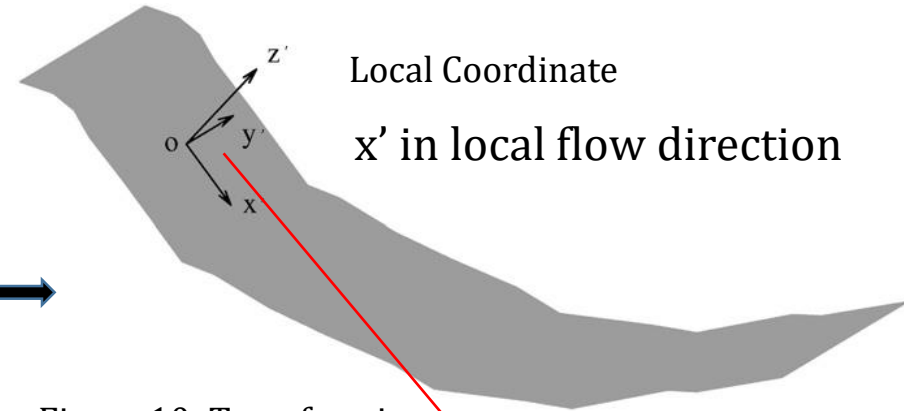
2. Shows no particular stress-strain rate relation, and inter-granular stresses satisfy the Coulomb rule;

3. Two coordinate systems:



$$\mathbf{C} = \begin{bmatrix} \frac{\bar{u}}{B} - \frac{D}{A^2 B} h_{s,x} & \frac{h_{s,y} \bar{w} - \bar{v}}{AB} & \frac{h_{s,x}}{A} \\ \frac{\bar{v}}{B} - \frac{D}{A^2 B} h_{s,y} & \frac{-h_{s,x} \bar{w} + \bar{u}}{AB} & \frac{h_{s,y}}{A} \\ \frac{\bar{w}}{B} - \frac{D}{A^2 B} & \frac{h_{s,x} \bar{v} - h_{s,y} \bar{u}}{AB} & \frac{1}{A} \end{bmatrix}$$

$$\mathbf{T}' = \mathbf{C}^T \cdot \mathbf{T} \cdot \mathbf{C}$$



4. In Local coordinates, only consider normal stress  $\tau_{ex'x'}$ ,  $\tau_{ey'y'}$  and  $\tau_{ez'z'}$  and dominant shear stresses  $\tau_{ez'x'}$  and  $\tau_{ex'z'}$ , and neglect other components.

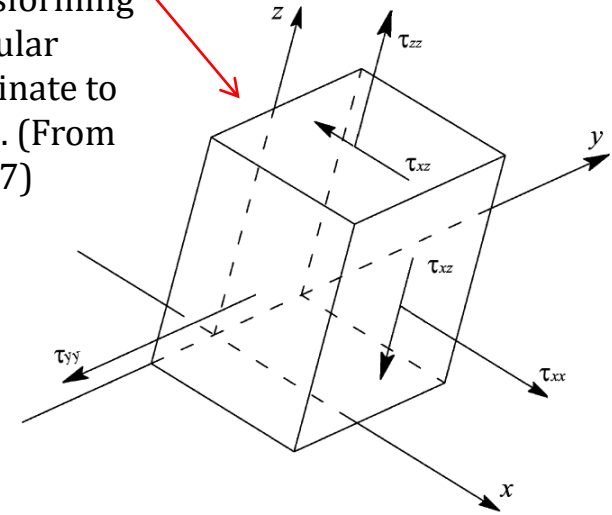
$$\tau_{ex'x'}(-h_s) = K_{x'act/pas} \cdot \tau_{ez'z'}(-h_s)$$

$$\tau_{ey'y'}(-h_s) = K_{y'act/pas} \cdot \tau_{ez'z'}(-h_s)$$

$$\tau_{ez'x'}(-h_s) = \tau_{ex'z'}(-h_s) = -\tau_{ez'z'}(-h_s) \cdot \tan \varphi_{bed}$$

$$\tau_{ez'y'}(-h_s) = \tau_{ey'z'}(-h_s) = \tau_{ex'y'}(-h_s) = \tau_{ey'x'}(-h_s) = 0$$

Figure 10: Transforming tensor from regular Cartesian coordinate to local coordinate. (From Pirulli et al. 2007)



## Numerical Approach

1. Governing equations in written in conservative form;
2. Two-step projection method used to update horizontal velocities;
3. TVD Finite volume scheme used to evaluate spatial derivatives;
4. Strong Stability Preserving (SSP) Runge-Kutta scheme used for time-stepping.;
5. Vertical velocity is determined using KBBC at bottom, and determined using z momentum equation at surface;
6. Non-hydrostatic pressure correction determined using a Poisson equation, and velocities updated in second step of projection scheme. (This step neglected in hydrostatic model)

$$\begin{aligned} & \left( \frac{L_{4,i,j}}{\Delta y^2} + \frac{L_{5,i,j}}{2\Delta y} \right) q_{b,i,j+1}^{n+1} + \left( \frac{L_{1,i,j}}{\Delta x^2} + \frac{L_{2,i,j}}{2\Delta x} \right) q_{b,i+1,j}^{n+1} + \left[ (L_3 + L_6 + L_7)_{i,j} - \frac{2L_{1,i,j}}{\Delta x^2} - \frac{2L_{4,i,j}}{\Delta y^2} \right] q_{b,i,j}^{n+1} \\ & + \left( \frac{L_{1,i,j}}{\Delta x^2} - \frac{L_{2,i,j}}{2\Delta x} \right) q_{b,i-1,j}^{n+1} + \left( \frac{L_{4,i,j}}{\Delta y^2} - \frac{L_{5,i,j}}{2\Delta y} \right) q_{b,i,j-1}^{n+1} = \text{RHS}_{i,j} \end{aligned}$$

# Verification and Validation

## 1. Tsunami generation by 2D submarine landslide (Grilli et al., 2017) :

Parameter:

$\Delta x = 0.01\text{m}$

9 sigma layers

CFL=0.5

Viscous model:

$\rho = 1,951\text{kg/m}^3$

$\mu_e = 0.01\text{ kg/(m.s)}$

Granular model:

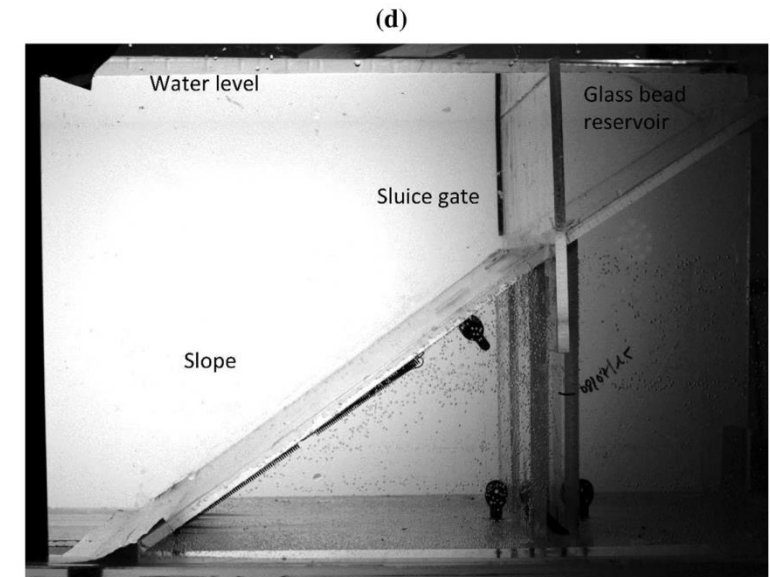
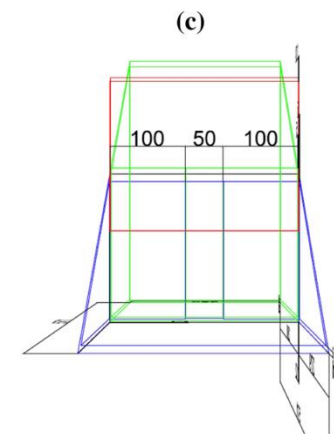
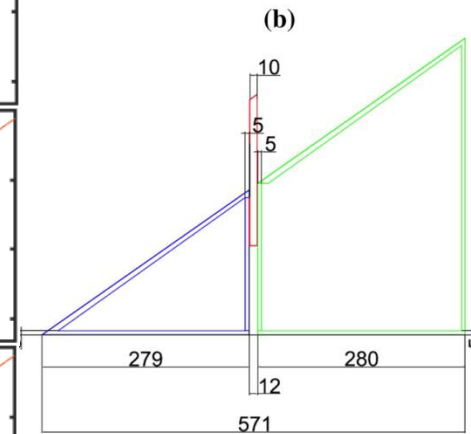
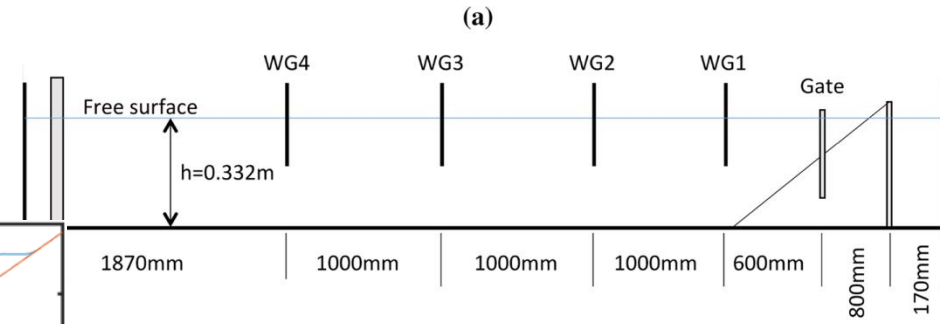
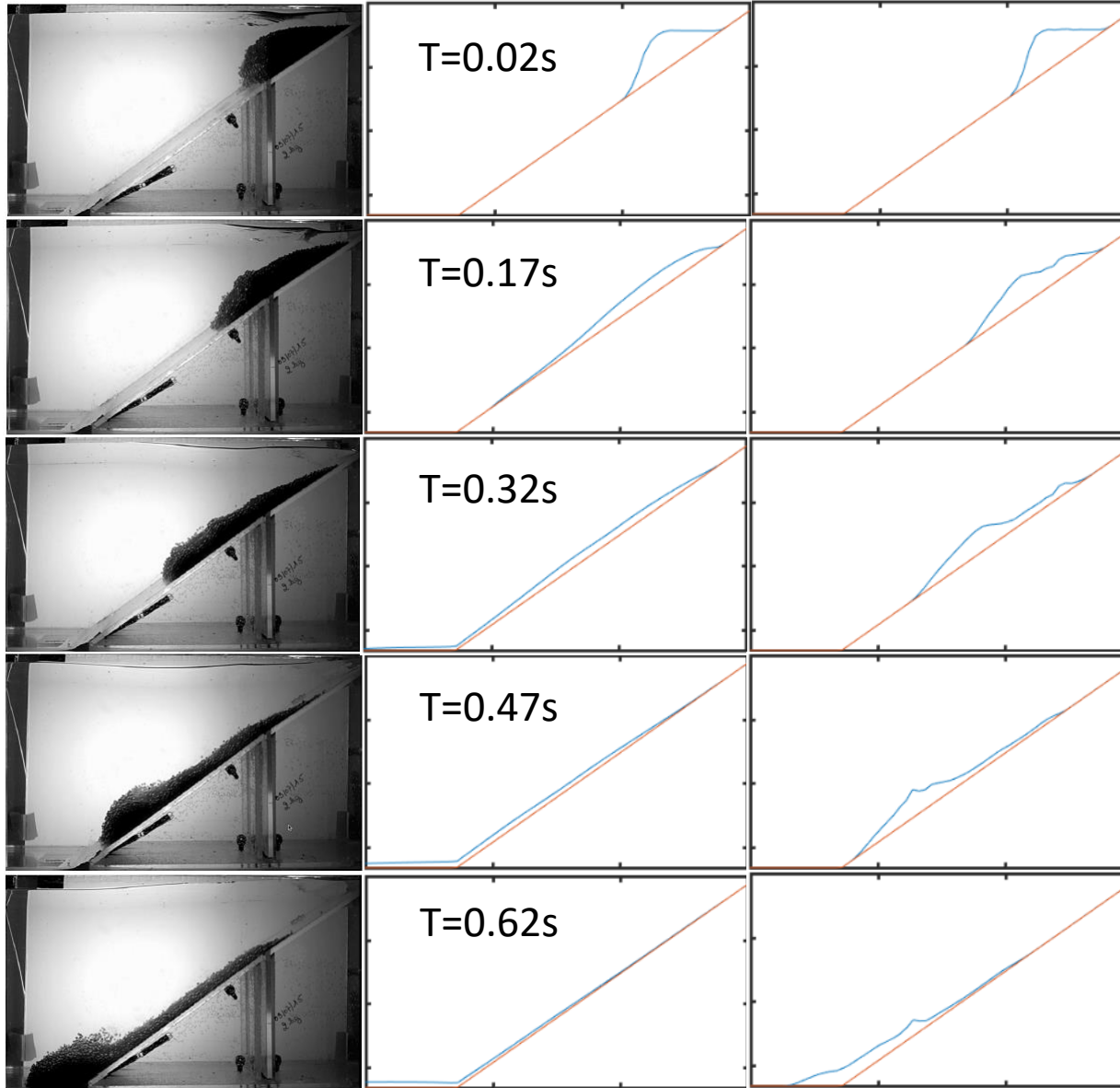
$\rho_s = 2,500\text{kg/m}^3$

$\rho_f = 1,000\text{kg/m}^3$

$\varphi = 63.4\%$

$\Phi_{\text{int}} = 34^\circ$

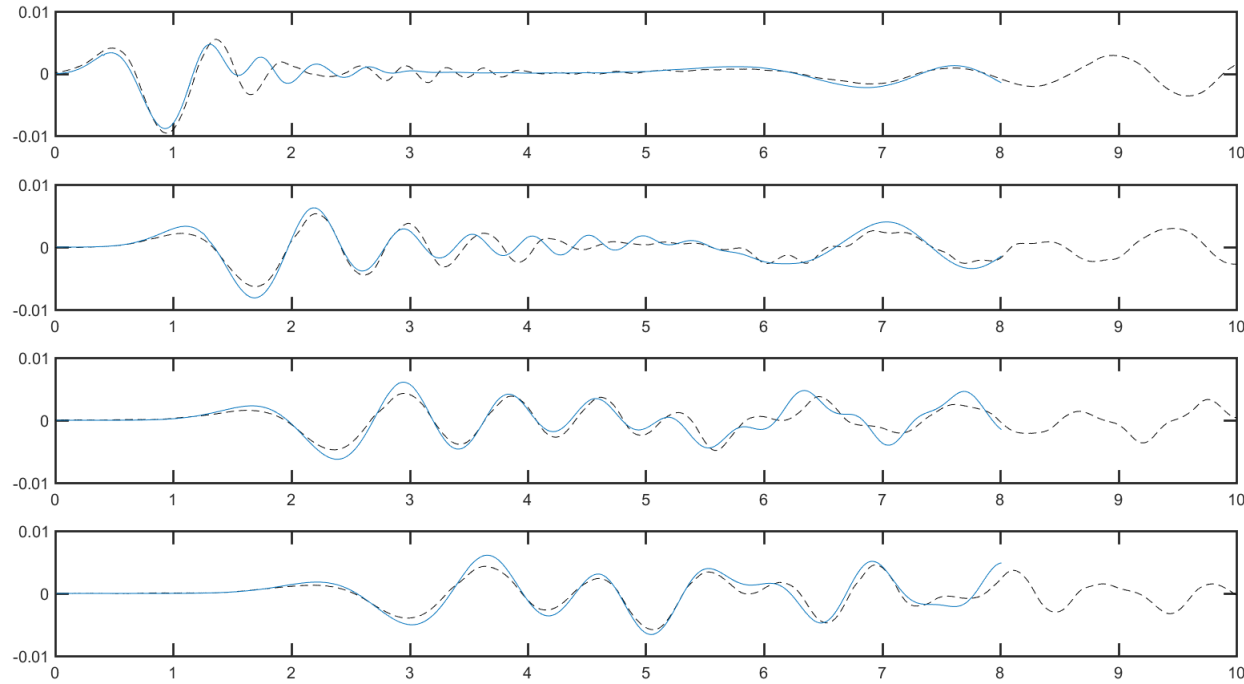
$\Phi_{\text{bed}} = 12^\circ$



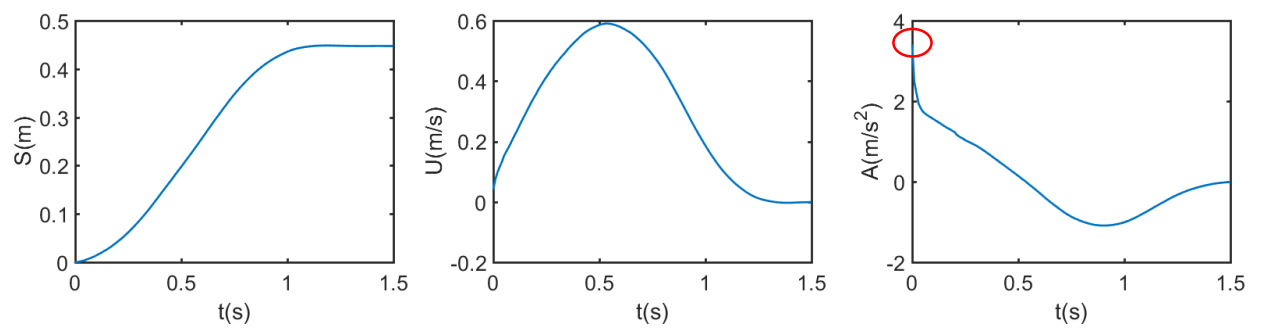
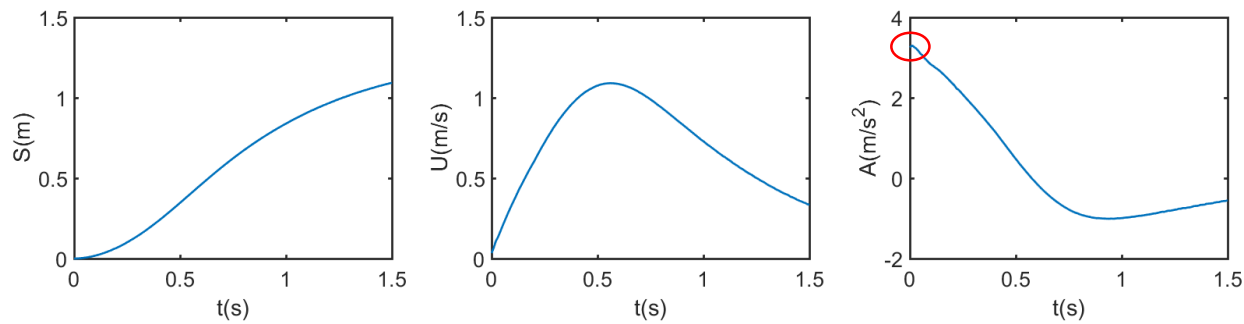
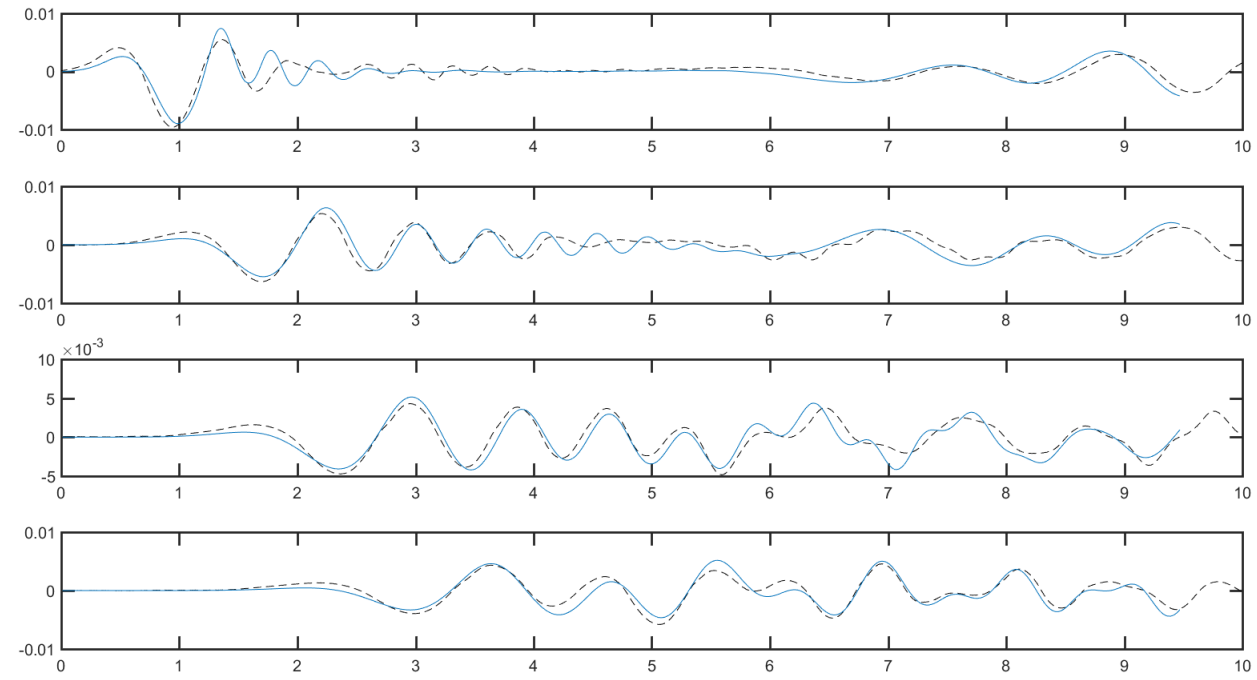
# Verification and Validation

## 2. Tsunami generation by 2D submarine landslide (Grilli et al., 2017) :

### Viscous model



### Granular model



# Verification and Validation

## 2. Tsunami generation by 2D subaerial landslide (Viroulet et al., 2014) :

Parameter:

$\Delta x = 0.005\text{m}$

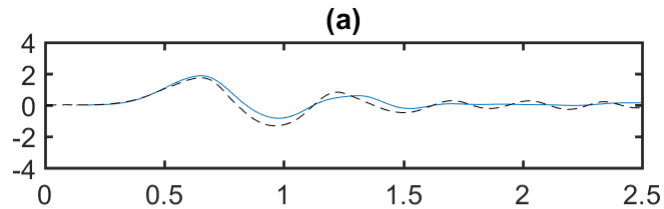
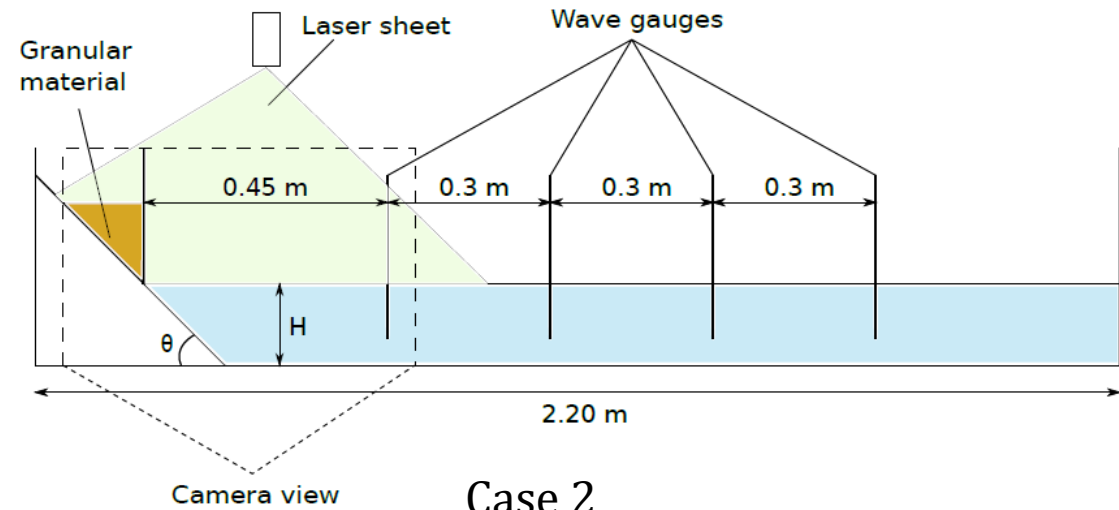
CFL = 0.5

$\rho_s = 2,500\text{kg/m}^3$

3 sigma layers

$\varphi = 60\%$

$\rho_f = 1,000\text{kg/m}^3$



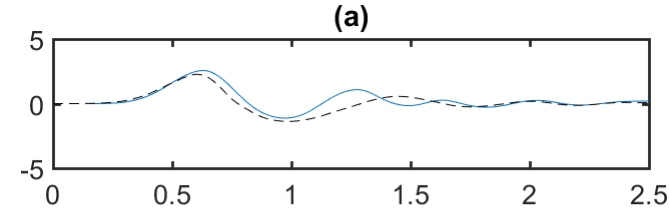
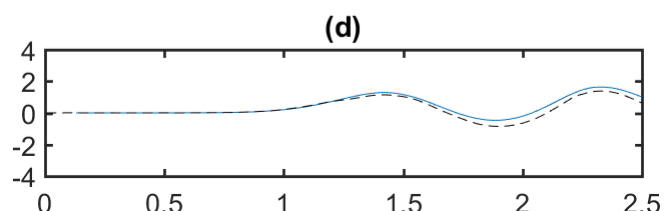
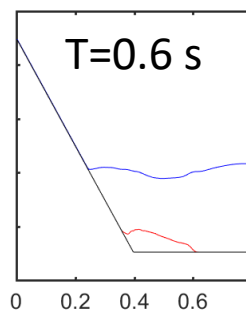
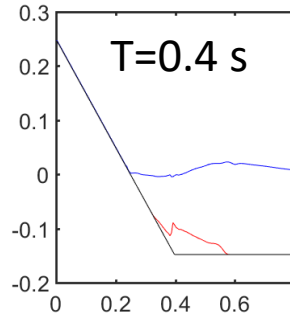
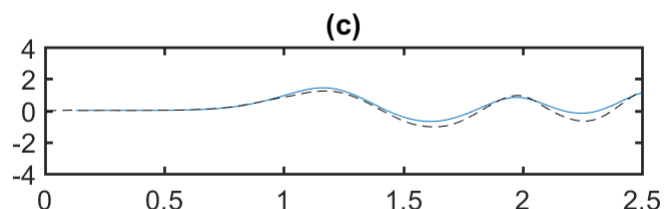
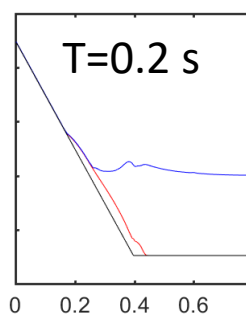
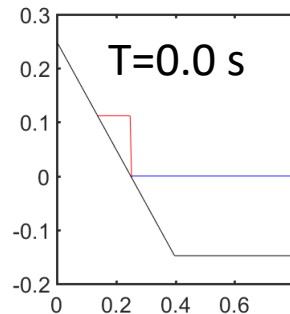
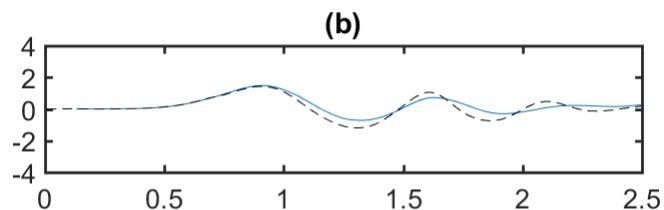
Case 1:

$H = 14.8\text{cm}$

$\Phi_{\text{int}} = 41^\circ$

$L = 11\text{cm}$

$\Phi_{\text{bed}} = 25.7^\circ$



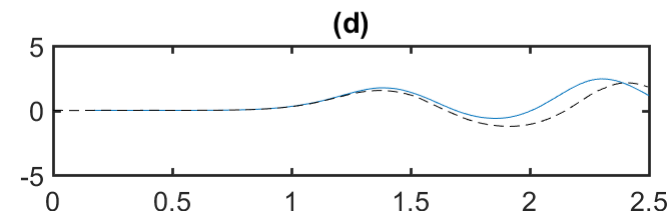
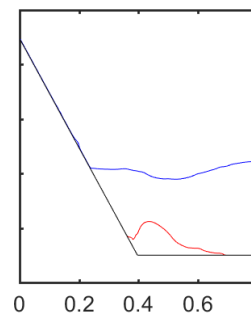
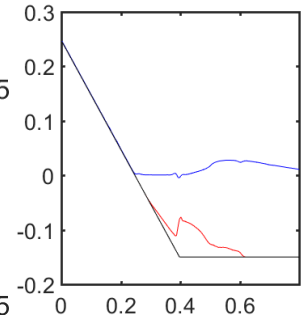
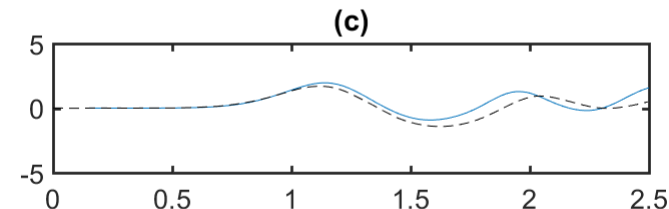
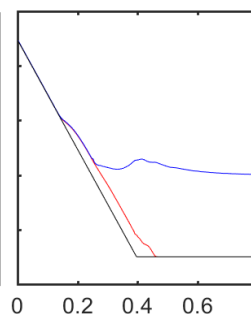
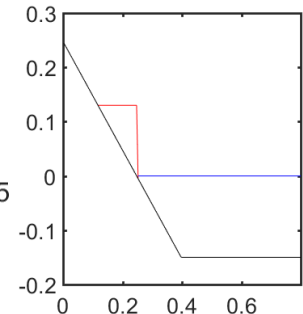
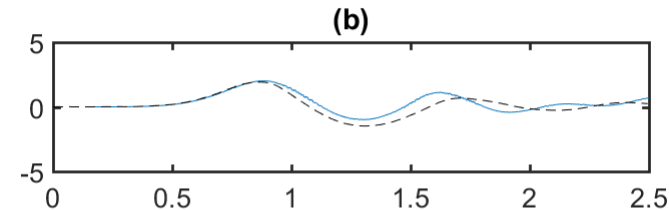
Case 2:

$H = 15\text{cm}$

$\Phi_{\text{int}} = 41^\circ$

$L = 13.5\text{cm}$

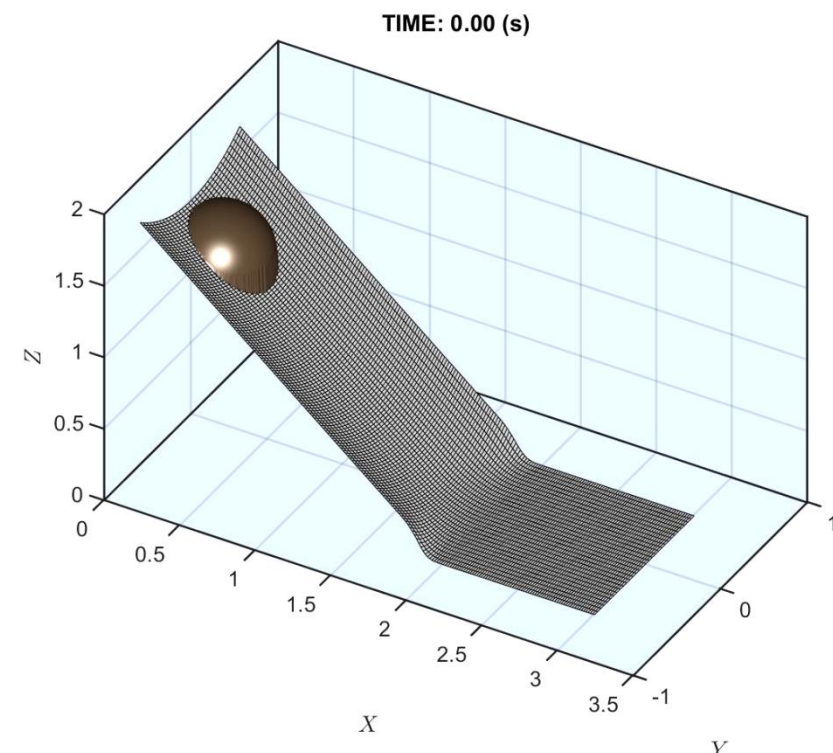
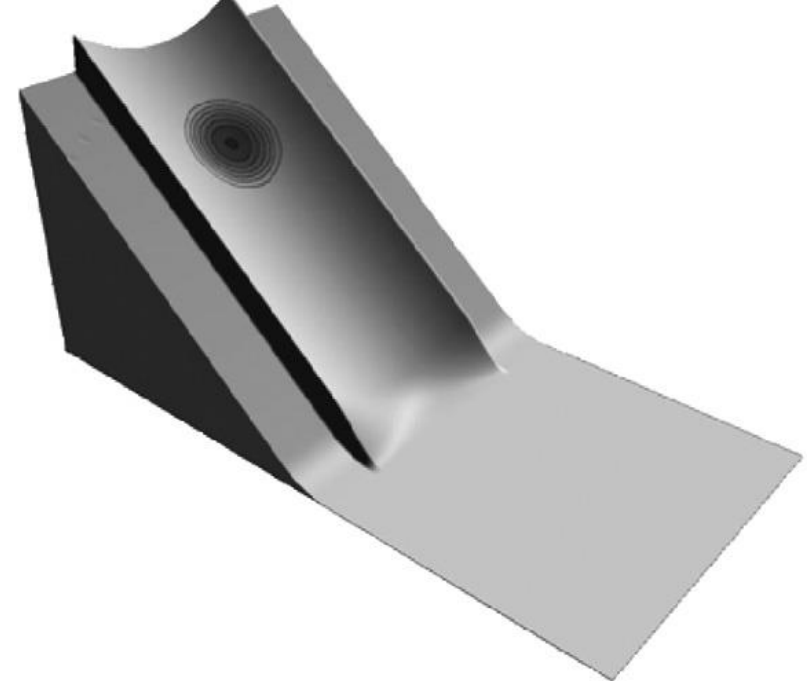
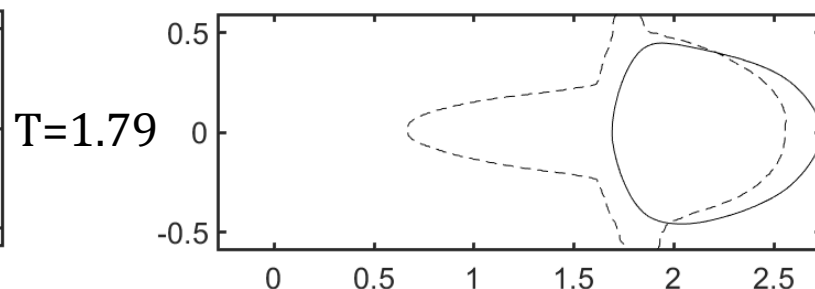
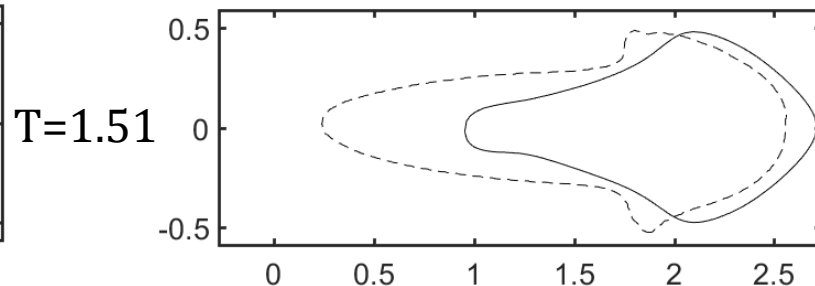
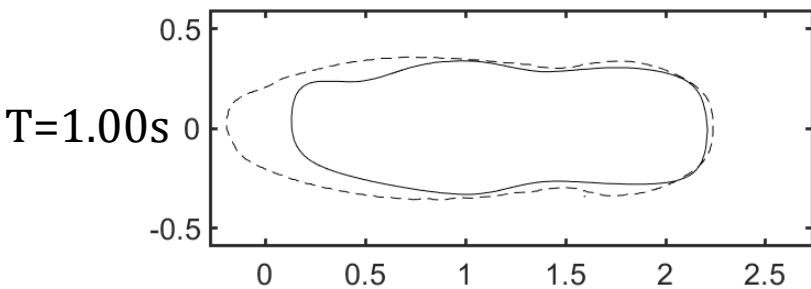
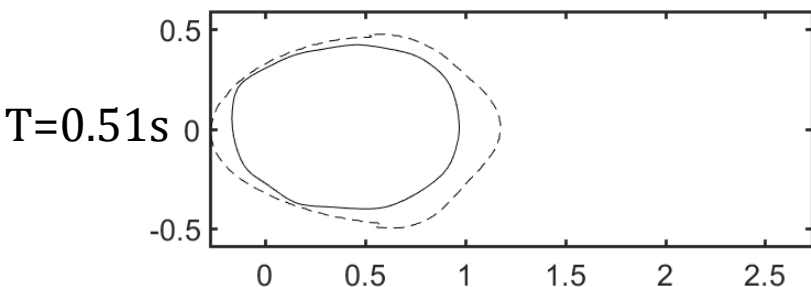
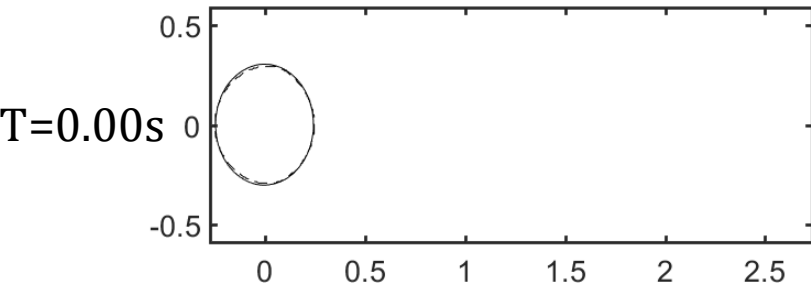
$\Phi_{\text{bed}} = 21.3^\circ$



# Verification and Validation

## 3. 3D granular flow move over irregular bathymetry (Gray et al., 1999) :

Parameter:  $\rho_s=2,500\text{kg/m}^3$   
 $\Delta x=0.0073658\text{m}$   $\rho_f=0\text{kg/m}^3$   
 $\Delta y=0.0073658\text{m}$   $\varphi = 60.0\%$   
CFL=0.5  $\Phi_{\text{int}}=40^\circ$   
 $\Phi_{\text{bed}}=30^\circ$



**Thank you!**

**Any questions?**

**A two-layer non-hydrostatic landslide model for tsunami generation  
on irregular bathymetry**

